Letter

Fingerprints of GeV scale right-handed neutrinos on inflationary gravitational waves and PTA data

Satyabrata Datta[1,2,*] and Rome Samanta[3,†]

[1]*Saha Institute of Nuclear Physics, 1/AF, Bidhannagar, Kolkata 700064, India*
[2]*Homi Bhabha National Institute, Second floor, BARC Training School Complex, Anushaktinagar, Mumbai, Maharashtra 400094, India*
[3]*CEICO, Institute of Physics of the Czech Academy of Sciences, Na Slovance 1999/2, 182 21 Prague 8, Czech Republic*

(Received 29 August 2023; accepted 2 November 2023; published 30 November 2023)

We show that the seesaw mechanisms that exhibit right-handed neutrino mass-dependent nonstandard postinflationary cosmology make blue-tilted inflationary gravitational waves (GWs) compatible with the recent findings of nanohertz stochastic GW background by the pulsar-timing arrays (PTAs) for high reheating temperatures. The right-handed neutrino (RHN) mass scale has to be $\mathcal{O}(\mathrm{GeV})$. Remarkably, such a scenario produces a correlated signature testable by the future LIGO run. In addition to contributing to the active neutrino masses, $\mathcal{O}(\mathrm{GeV})$ RHNs generate baryon asymmetry of the Universe via low scale leptogenesis. They can be searched for in collider experiments. Therefore, the recent detection by PTAs is not only exciting for GWs in the nanohertz range, it paves the way to test and constrain well-studied mechanisms, such as seesaws, with a low frequency and a correlated measurement of high-frequency GW spectral features, complementary to particle physics searches.

DOI: 10.1103/PhysRevD.108.L091706

Introduction. Recently, pulsar-timing array (PTA) collaborations—NANOGrav, EPTA, and PPTA, along with the InPTA and CPTA—have released their latest data asserting significant evidence for a stochastic gravitational wave background (SGWB) at nanohertz frequencies [1–4]. Such a finding, albeit with less statistical significance, has already been there for the last two years, creating a reasonable buzz within the scientific community [5–7]. This time, however, the signal exhibits the characteristic pulsar angular correlations, known as the quadrupolar Hellings-Downs curve [8], which is unique to an SGWB. While the sources of such gravitational waves (GWs) remain unknown, the preferred power law $\Omega_{\mathrm{GW}} \propto f^{1.8\pm0.6}$, e.g., in the NANOGrav new data do not disfavor the simple GW-driven models of supermassive black hole binaries at 3σ. Another exciting possibility, nonetheless, is to investigate GWs of cosmological origin. In a companion theory paper [9], the NANOGrav Collaboration (for definiteness, we shall focus on NANOGrav 15 yr data [1]; results of other PTAs are in good agreement) produced an exhaustive catalog discussing plenty of cosmological sources that comply with the data.[1] Subsequently, in various articles, such sources were discussed either in the context of different cosmological models or reperforming the fit to the new data, including the results of other PTAs [16–34]. An inflationary gravitational wave with large tensor blue tilt [henceforth, we address them as blue-tilted gravitational waves (BGWs)] is one that provides an excellent fit to the old as well as the new data [1,6,35–39]; though, it should be noted that such BGWs can be produced in models that, in general, do not correspond to standard slow-roll inflation, see, e.g., [40–47]. The parameter space of such a fit is, however, restrictive. This is because GWs with large blue tilt, considering the spectrum is still a power law at higher frequencies, saturate big bang nucleosynthesis (BBN) bound on the effective number of neutrino species, disfavoring any postinflationary cosmology founded on high reheating temperature ($T_{\mathrm{RH}} \gtrsim 10\,\mathrm{GeV}$) after inflation [9,39]. Nonetheless, if a nonstandard matter epoch leads to entropy production between the reheating after inflation and the most recent radiation domination before the BBN [48], BGWs get suppressed and provide a good fit to PTA data for high reheating temperatures. Now, contrary to the standard case, such a scenario allows the overall GW spectrum to

*satyabrata.datta@saha.ac.in
†romesamanta@gmail.com

[1]Unlike the 12.5 yr NANOGrav data, for which stable cosmic strings provide a good fit [10–15], the recent data disfavor stable cosmic strings [1].

span decades of frequencies with characteristic spectral features testable, e.g., by the LIGO [49,50].

In this Letter, we show the seesaw mechanisms with GeV scale right-handed neutrinos (RHNs), which are now being extensively discussed within the context of low-mass sterile neutrino searches (see a review: [51]), naturally provide an RHN mass-dependent matter epoch to fit the PTA data with BGWs (we shall see later that a high $T_{\rm RH}$ is also a requirement of the model). The scenario correlates RHN masses with the amplitude and spectral features in the BGWs verifiable at high-frequency GW detectors, providing a novel synergic search for GeV scale RHNs, which, in addition to generating active neutrino masses via seesaw, also offer successful baryogenesis via low scale leptogenesis [52–55].

The theoretical framework is founded primarily on this question: What is the origin of small (here GeV) RHN masses? Although the electroweak naturalness condition puts an upper bound on the RHN masses, $M_i < 10^7$ GeV [56,57], generally, in GeV scale seesaw scenarios, the origin of such small RHN masses are not addressed; they are considered to be the bare masses in the theory. Nonetheless, the seesaw Lagrangian provides all the degrees of freedom if we suppose RHN masses originate from a phase transition driven by a scalar field [58,59]. In which case, the RHN field N couples to a scalar field Φ as $\mathcal{L} \sim f_N N N \Phi$ (omitting family indices), with f_N being a Yukawa coupling. After the phase transition, Φ obtains its vacuum expectation value v_Φ and generates RHN mass as $M = f_N v_\Phi$. On the other hand, if kinematically allowed, Φ can decay to a pair of RHNs ($\Phi \to NN$), with the decay rate $\Gamma \propto f_N^2$. RHN masses and the decay width (or lifetime) of Φ are now connected via f_N. For a fixed v_Φ (which may be large), one obtains a required small value of M for a small f_N, making Φ long-lived. We shall see that the long-lived Φ dominates the Universe's energy budget as a matter component before decaying. The smaller the M, the longer the lifetime of Φ. This results in a longer duration of matter domination—hence, larger entropy production and more suppressed BGWs. The time and amount of entropy production correlate the amplitude and spectral features of BGWs with RHN mass scale M. For more technical details, please see Ref. [59] where the idea explained above was introduced.

RHN mass-dependent matter domination. Obtaining RHN masses via a phase transition is not *ad hoc*; the coupling $f_N N N \Phi$ can appear as $\mathrm{U}(1)_{B-L}$ symmetric coupling following the breaking of a grand unification group [60–63]. In that case, N and Φ have $B-L$ charge 1 and -2, respectively. Therefore, for concreteness, we shall consider a $B-L$ phase transition; i.e., as the temperature drops, the scalar field rolls from $\Phi = 0$ toward $\Phi = v_\Phi$, breaking the $B-L$ symmetry. The finite temperature potential that restores the symmetry at higher temperatures is given by [64,65]

$$V(\Phi, T) = \frac{\lambda}{4}\Phi^4 + D(T^2 - T_0^2)\Phi^2 - ET\Phi^3, \qquad (1)$$

where D, E, and T_0 are functions of gauge coupling g', the self-interaction coupling λ, and $v_\Phi = \frac{\mu}{\sqrt{\lambda}}$ determined from the zero temperature potential $V(\Phi, 0) = -\frac{\mu^2}{2}\Phi^2 + \frac{\lambda}{4}\Phi^4$ [59]. The last term in Eq. (1) generates a potential barrier, causing a secondary minimum at $\Phi \neq 0$, which at $T = T_c$ degenerates with the $\Phi = 0$ one. The potential barrier vanishes at $T_0 (\lesssim T_c)$, making the minimum at $\Phi = 0$ a maximum. The critical temperature T_c and the field value $\Phi_c \equiv \Phi(T_c)$ are given by [59]

$$T_c = T_0 \frac{\sqrt{\lambda D}}{\sqrt{\lambda D - E^2}}, \qquad \Phi_c = \sqrt{\frac{4D}{\lambda}(T_c^2 - T_0^2)}. \qquad (2)$$

The transition dynamics can be described as a rolling of Φ if it smoothly transits to $\Phi = v_\Phi$, which can be quantified roughly with the order parameter $\Phi_c/T_c \ll 1$. In this case, the field rolls because the potential barrier disappears very quickly [58,59]. The condition $\Phi_c/T_c \ll 1$ can be fulfilled for $\lambda \simeq g'^3$ and $g' \lesssim 10^{-2}$, which correspond to $\Phi_c/T_c \lesssim 0.08$ [59]. Once it rolls down, the field oscillates around v_Φ. For $V(\Phi) = \alpha \Phi^\beta$, the equation of state of such an oscillation phase is computed as $\omega = (\beta - 2)(\beta + 2)^{-1}$ [59]. Assuming the oscillation of the scalar field is driven by the dominant quadratic term in the potential and expanding the zero temperature potential around v_Φ, we obtain $\alpha = \lambda v_\Phi^2$ and $\beta = 2$. Therefore, the scalar field behaves like matter ($w = 0$). One can also compute the angular frequency of oscillation as $m_\Phi = \sqrt{2\lambda} v_\Phi$.

The decay channels determine the lifetime of Φ. For $\lambda \simeq g'^3$ and $g' \ll 1$, $\Phi \to z' z'$ is not allowed from kinematic consideration. Here z' is the $\mathrm{U}(1)_{B-L}$ gauge boson. Another decay mode $\Phi \to hh$, where h is the standard model (SM) Higgs boson, does not contribute if Φ is sequestered from SM Higgs at the tree level (even at the radiative level, it is not efficient due to the discussed small values of f_N). Then, the competing decay channels are $\Phi \to NN$ and $\Phi \to f\bar{f}V$ (the corresponding two-body decay; $\Phi \to f\bar{f}$ is suppressed due to chirality flip, e.g., [66]), where f and V are SM fermions and vector bosons. The former corresponds to a tree-level process, whereas the latter is a one-loop ($z' z' f$) triangle process. The strengths of these two processes are determined by the couplings f_N and g'. To control the duration of matter domination with small RHN mass via f_N, the process $\Phi \to NN$ should dominate ($\Gamma_N^\Phi \gtrsim \Gamma_{f\bar{f}V}$). In which case, the entropy produced (κ) by the decay of Φ is given by (which amounts typically equivalent to the ratio of the temperatures corresponding to the time when Φ dominates and when it decays, see, e.g., the Supplemental Material [67]) [59]

$$\kappa^{-1} \simeq \frac{\left(\frac{90}{\pi^2 g_*}\right)^{1/4} \rho_R(T_c) \sqrt{\Gamma_N^\Phi \tilde{M}_{\rm Pl}}}{\rho_\Phi(T_c) T_c}, \tag{3}$$

where $\tilde{M}_{\rm Pl} = 2.4 \times 10^{18}$ GeV is the reduced Planck constant, $\rho_\Phi(T_c) \equiv V_{\rm eff}(0, T_c) \simeq \frac{\lambda}{4} v_\Phi^4$, g_* is energy degrees of freedom, and $\Gamma_N^\Phi \simeq \frac{f_N^2}{10\pi} m_\Phi$. The analytical formula for κ is very precise, and we shall use it to compute the GW spectrum. Let us mention the following conditions that the model complies with. (i) As mentioned, $\Gamma_N^\Phi \gtrsim \Gamma_{f\bar{f}V}$, (ii) Φ decays before BBN ($T \sim 5$ MeV), (iii) the transition happens following reheating after inflation, i.e., $T_c \lesssim T_{\rm RH}$, and (iv) the vacuum energy does not dominate the radiation at T_c [$\rho_\Phi(T_c) < \rho_R(T_c)$]; the violation of which leads to a second period of inflation. We shall see shortly that there are three additional constraints, excluding the PTA data, and the model has six free parameters. Therefore, the model withstands with 6:8 capacity against the constraints (including PTA data), leading to extremely robust predictions. Specifically, we shall see that the recent PTA data can be explained only for a constrained range of RHN masses, which can be probed by the future LIGO run and is also interesting for future collider FCC-ee.

Fit to the NANOGrav data and predictions. GWs are described with the perturbed Friedmann-Lemaître-Robertson-Walker line element,

$$ds^2 = a(\tau)[-d\tau^2 + (\delta_{ij} + h_{ij}) dx^i dx^j)], \tag{4}$$

where τ is the conformal time, and $a(\tau)$ is the scale factor. The transverse and traceless part of the 3×3 symmetric matrix h_{ij}, $\partial_i h^{ij} = 0$ and $\delta^{ij} h_{ij} = 0$, characterizes the GWs. Following the linearized evolution equation

$$\partial_\mu(\sqrt{-g}\partial^\mu h_{ij}) = 16\pi a^2(\tau)\pi_{ij}, \tag{5}$$

considering subdominant contribution from anisotropy stress tensor π_{ij} [68], and solving the Fourier space propagation equation for h_{ij}, one obtains the gravitational wave energy density as [69]

$$\Omega_{\rm GW}(k) = \frac{1}{12H_0^2}\left(\frac{k}{a_0}\right)^2 T_T^2(\tau_0, k) P_T(k), \tag{6}$$

where $H_0 \simeq 2.2 \times 10^{-4}$ Mpc^{-1} and $\tau_0 = 1.4 \times 10^4$ Mpc. The quantity $P_T(k)$ represents the primordial power spectrum connecting to the inflation models,

$$P_T(k) = r A_s(k_*)\left(\frac{k}{k_*}\right)^{n_T}, \tag{7}$$

where $r \lesssim 0.06$ [70] [constraint (v)] is the tensor-to-scalar-ratio, $k = |\vec{k}| = 2\pi f$ with f being the frequency of the GWs at the present time at $a_0 = 1$, $A_s \simeq 2 \times 10^{-9}$ is the scalar perturbation amplitude at the pivot scale $k_* = 0.01$ Mpc^{-1}, and n_T is the tensor spectral index. The simplest single-field slow-roll inflation models satisfy a consistency relation: $n_T = -r/8$ [71]. We shall treat $n_T > 0$ as constant, ignoring scale dependence due to higher-order corrections [72]. The most important quantity in the discussion is the transfer function $T_T(\tau_0, k)$ given by [73–78]

$$T_T^2(\tau_0, k) = F(k) T_1^2(\zeta_{\rm eq}) T_2^2(\zeta_\Phi) T_3^2(\zeta_{\Phi R}) T_2^2(\zeta_R), \tag{8}$$

where $F(k)$ reads

$$F(k) = \Omega_m^2 \left(\frac{g_*(T_{k,\rm in})}{g_{*0}}\right)\left(\frac{g_{*s0}}{g_{*s}(T_{k,\rm in})}\right)^{4/3}\left(\frac{3 j_1(k\tau_0)}{k\tau_0}\right)^2, \tag{9}$$

with $j_1(k\tau_0)$ being the spherical Bessel function, $\Omega_m = 0.31$, $g_{*0} = 3.36$, and $g_{*0s} = 3.91$. We use the scale-dependent $g_{*0(s)}(T_{k,\rm in})$ in Eq. (9) from [78–80], where $T_{k,\rm in}$ is the temperature corresponding to the horizon entry of kth mode. The $T_i(\zeta)$'s are given by

$$T_1^2(\zeta) = 1 + 1.57\zeta + 3.42\zeta^2, \tag{10}$$

$$T_2^2(\zeta) = (1 - 0.22\zeta^{1.5} + 0.65\zeta^2)^{-1}, \tag{11}$$

$$T_3^2(\zeta) = 1 + 0.59\zeta + 0.65\zeta^2, \tag{12}$$

where $\zeta_i \equiv k/k_i$, with k_i's being the modes

$$k_{\rm eq} = 7.1 \times 10^{-2} \Omega_m h^2 {\rm Mpc}^{-1}, \tag{13}$$

$$k_\Phi = 1.7 \times 10^{14}\left(\frac{g_{*s}(T_\Phi)}{106.75}\right)^{1/6}\left(\frac{T_\Phi}{10^7\ {\rm GeV}}\right)\ {\rm Mpc}^{-1}, \tag{14}$$

$$k_{\Phi R} = 1.7 \times 10^{14} \kappa^{2/3}\left(\frac{g_{*s}(T_\Phi)}{106.75}\right)^{1/6}\left(\frac{T_\Phi}{10^7\ {\rm GeV}}\right)\ {\rm Mpc}^{-1}, \tag{15}$$

$$k_R = 1.7 \times 10^{14} \kappa^{-1/3}\left(\frac{g_{*s}(T_{\rm RH})}{106.75}\right)^{1/6}\left(\frac{T_{\rm RH}}{10^7\ {\rm GeV}}\right)\ {\rm Mpc}^{-1}, \tag{16}$$

crossing the horizon at standard matter-radiation equality temperature $T_{\rm eq}$, at $T_\Phi \simeq \left(\frac{90}{\pi^2 g_*}\right)^{1/4}\sqrt{\Gamma_N^\Phi \tilde{M}_{\rm Pl}}$ when Φ decays, at $T_{\Phi R}$ when Φ dominates the energy density, and at $T_{\rm RH}$, respectively. Given the above set of equations and using κ from Eq. (3), we evaluate Eq. (6) to obtain the GW spectrum and to fit the NANOGrav data, considering two more constraints: (vi) LIGO bound on SGWB, which roughly reads $\Omega_{\rm GW}(35\ {\rm Hz})h^2 \leq 6.8 \times 10^{-9}$ [49], and (vii) BBN bound on the effective number of neutrino species: $\int_{f_{\rm low}}^{f_{\rm high}} f^{-1} df \Omega_{\rm GW}(f) h^2 \lesssim 5.6 \times 10^{-6} \Delta N_{\rm eff}$, where

$\Delta N_{\rm eff} \lesssim 0.2$ [81]. $f_{\rm low}$ corresponds to the frequency entering the horizon during BBN epoch. On the other hand, the Hubble rate at the end of inflation determines the upper limit: $f_{\rm high} = a_{\rm end} H_{\rm end}/2\pi$. For numerical computations, $f_{\rm high} \simeq 10^5$ Hz would suffice because the spectrum falls and the integration saturates. We follow the NANOGrav parametrization for the GW energy density to perform a power-law fit to the new data within the frequency range $f \in [10^{-9}\ \text{Hz}, f_{\rm yr}]$. The parametrization reads

$$\Omega_{\rm GW}(f) = \Omega_{\rm yr}\left(\frac{f}{f_{\rm yr}}\right)^{(5-\gamma)}, \tag{17}$$

with $\Omega_{\rm yr} = \frac{2\pi^2}{3H_0^2} A^2 f_{\rm yr}^2$ and $f_{\rm yr} = 1\ \text{yr}^{-1} \simeq 32$ nHz. Fitting the data requires comparing Eqs. (6) and (17), then extracting the values of the amplitude A and the spectral index γ that lie within the $1\sigma, 2\sigma$, and 3σ contours (cf. middle panel of Fig. 1) reported by the NANOGrav [1]. In the left panel of Fig. 1, we show a GW spectrum consistent with all the constraints. To produce the figure, the following benchmark values for the model parameters have been used: $T_{\rm RH} = 10^{13}$ GeV, $n_T = 0.9$, $r = 0.06$, $v_\Phi = 10^{14}$ GeV, $g' = 10^{-2.9}$, and $M = 16$ GeV. The corresponding values of A and γ are shown in the middle panel with the red star. The fit is not very different from the standard BGW fit without intermediate matter domination [39]. This is because, within the NANOGrav frequency range, the transfer function $T_1(\zeta)$ determines the spectral shape, which results in $\gamma \sim 5 - n_T \simeq 4$. Note also that the first peak of the spectrum occurs at a frequency $f_\Phi > f_{\rm yr}$ so that the NANOGrav band can be fitted with a pure power law $\Omega_{\rm GW}(f \lesssim f_{\rm yr}) \sim f^{n_T}$. An analytical expression for f_Φ can be derived from Eq. (14), which is given by

$$f_\Phi \simeq 50\ \text{nHz}\left(\frac{M}{16\ \text{GeV}}\right)\left(\frac{10^{14}\ \text{GeV}}{v_\Phi}\right)^{1/2}\left(\frac{g'}{10^{-2.9}}\right)^{3/4}. \tag{18}$$

One can do a more exhaustive fit by varying the parameters. For instance, in the right panel, we varied g' and M, keeping the rest fixed to their benchmark values. Nonetheless, there is no qualitative difference—allowed values of the other parameters lie near the benchmarks. This does not change significantly even though one varies all the parameters. As stated earlier, this is because of a bunch of constraints with which the model complies. Among all the constraints, the first, i.e., $\Gamma_N^\Phi \gtrsim \Gamma_{f\bar{f}\nu}$, the third, i.e., $T_{\rm RH} \gtrsim T_c$, and the sixth, i.e., LIGO bound on SGWB, are much stronger, making the allowed parameter space consistent with the NANOGrav data stringent. This model fits the NANOGrav data at 2σ with $M \in [1, 47]$ GeV for random values of other parameters around the benchmark and without violating any constraints. Remarkably, consistency with the NANOGrav data makes the model extremely predictive, not only in terms of RHN masses; the infrared tail of the second peak in the GW spectrum passes through the sensitivity region of advanced LIGO (aLIGO), for a significant portion of allowed parameter space (see the right panel in Fig. 1). Therefore, any nonobservation of SGWB by aLIGO would potentially rule out a large parameter space of the model, *provided* that the model fits NANOGrav data. Not only that, the latter also motivates us to combine, for the first time, the particle physics sensitivity curves for GeV scale RHN searches with the aLIGO projection, shown in Fig. 2 with the vertical sky-blue band representing the RHN mass range $M \in [2.5, 47]$ GeV. Particle physics experiments are

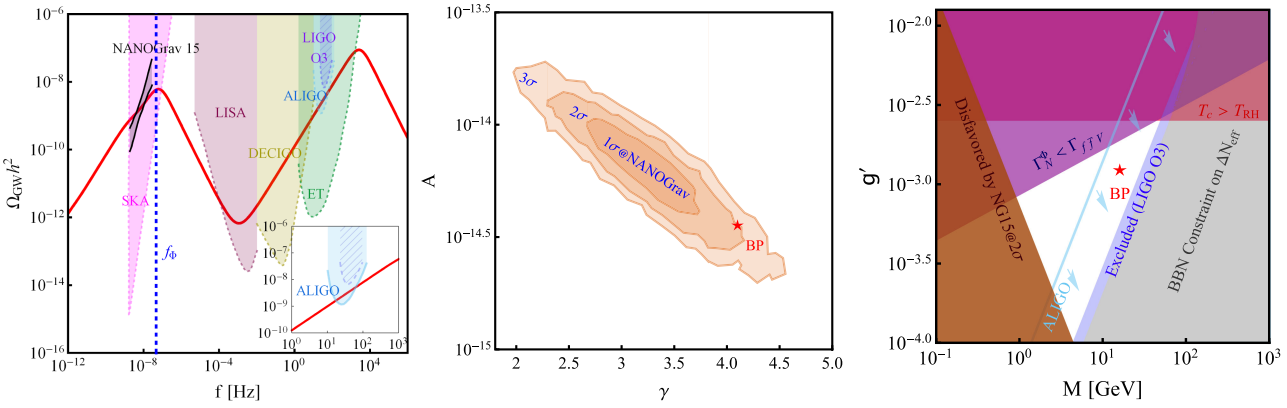

FIG. 1. Left: the spectrum has been generated for $M = 16$ GeV. For other benchmarks, please see the text. Besides NANOGrav and LIGO, sensitivities of SKA [82], LISA [83], DECIGO [84], and ET [85] are shown. The vertical dashed blue line represents the frequency corresponding to Eq. (18). Middle: the red ⋆ represents the fit point corresponding to the GW spectrum on the left. BP stands for benchmark point. Right: an allowed parameter space on the $g' - M$ plane (white). All the colored regions are excluded. The NANOGrav signal cannot be reproduced in the brown region at 2σ. BBN constraint on $\Delta N_{\rm eff}$ disfavors the gray region. The LIGO-O3 bound on SGWB excludes the purple region. The region right to the sky-blue line (indicated by arrows) represents the future aLIGO sensitivity. In the pink region (top left corner), the three-body decay of Φ is more dominant than the right-handed (RH) neutrino pair production. In the red region on the top, one has $T_c > T_{\rm RH}$.

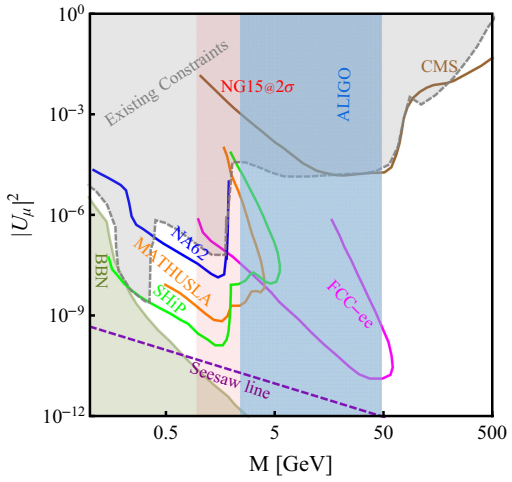

FIG. 2. Particle physics exclusion and projections for RHN mixing with muon flavor. The gray region and region above the brown curve are excluded from the previous experiments and CMS 13 TeV run [51,86,87]. Future sensitivities of SHiP [88], MATHUSLA [89], NA62 [90], and FCC-ee [91] are shown with green, orange, blue, and pink curves. The region named BBN is excluded; otherwise, the decay product of RHNs would contradict BBN prediction. The dashed line represents the mixing in the canonical seesaw $|U_\mu|^2 \sim m_\nu/M$. The vertical red band represents the RHN mass range $M \sim [1, 47]$ GeV consistent with NANOGrav 2σ data. The vertical sky-blue band represents the RHN mass range $M \sim [2.5, 47]$ GeV consistent with NANOGrav 2σ data and testable with SGWB searches by advanced LIGO.

sensitive to RHN masses and their mixing ($|U_\alpha|^2 \sim m_\nu/M$) to active neutrinos, where m_ν is the active neutrino mass scale ($\simeq$0.05 eV). On the contrary, predictions of this model depend on the former, allowing us to identify the region independent of $|U_\mu|$ in Fig. 2.

We conclude with the following remarks covering some additional aspects of the work. (1) The framework can be extended to other variants, such as inverse seesaw, which offers additional phenomenology. (2) One may straightforwardly obtain analytical expressions of the peak and dip frequencies in terms of RHN masses using Eqs. (14)–(16) (via T_Φ). (3) We do not present explicit computation of leptogenesis. It would be interesting to reproduce calculations, e.g., of [55] (including entropy production), leading to a parameter space sensitive to $|U_\alpha|$ and M. (4) This one is perhaps the most interesting: the possibility of obtaining GWs from cosmic strings. The occurrence of $B-L$ phase transition would naturally produce cosmic gauge strings. We, however, work with unconventional values of λ and g', which, in general, are taken as $\mathcal{O}(1)$ in the Nambu-Goto simulations [92–94]. Additionally, for the parameter space consistent with the NANOGrav data, the cosmic string width $\delta_w \sim 1/\sqrt{\lambda} v_\Phi$ constitutes a considerable fraction of the horizon $H(T_c)^{-1}$ (relatively thick strings). Claiming GWs from cosmic strings in this model thus requires a straightforward assumption (which we are less confident about): results of the numerical simulations also hold for our preferred parameter range. An existence of GWs from cosmic strings, nonetheless, would produce further spectral distortion to the BGWs shown in Fig. 1, making a combined peak-plateau-peak spectrum instead of a peak-dip-peak one (see the Supplemental Material [67]). This distinguishes the model from any other matter domination + BGW scenario, even at the level of the GW spectrum.

Summary. We discuss a novel framework to probe seesaw models with GeV scale RHNs with the recent PTA data interpreted as SGWB from inflation. A fit to the PTA data with inflationary GWs predicts the mass scale of RHNs to be $\mathcal{O}$(GeV) and a PTA-LIGO correlation on SGWB. While any nonobservation of SGWB by aLIGO would rule out a large parameter space of the model, the recent PTA data motivate us to combine the particle physics sensitivity curves for low-mass RHN searches with the future LIGO projection for the mass range $M \sim [2.5, 47]$ GeV. We performed the fit with the NANOGrav 15 yr data. We do not expect a significant qualitative change in our results if the fit is performed by combining the data from all the PTAs, because the $A-\gamma$ global contours reported by the IPTA Collaboration are similar [95] to the NANOGrav ones.

Acknowledgment. R. S. is supported by the project International Mobility MSCA-IF IV FZU—CZ.02.2.69/0.0/0.0/20_079/0017754 and acknowledges European Structural and Investment Fund and the Czech Ministry of Education, Youth, and Sports.

[1] G. Agazie *et al.* (NANOGrav Collaboration), Astrophys. J. Lett. **951**, L8 (2023).
[2] J. Antoniadis, P. Arumugam, S. Arumugam, S. Babak, M. Bagchi, A. S. B. Nielsen, C. G. Bassa, A. Bathula, A. Berthereau, M. Bonetti *et al.*, Astron. Astrophys. **678**, A50 (2023).
[3] D. J. Reardon, A. Zic, R. M. Shannon, G. B. Hobbs, M. Bailes, V. Di Marco, A. Kapur, A. F. Rogers, E. Thrane, J. Askew *et al.*, Astrophys. J. Lett. **951**, L6 (2023).
[4] H. Xu, S. Chen, Y. Guo, J. Jiang, B. Wang, J. Xu, Z. Xue, R. N. Caballero, J. Yuan, Y. Xu *et al.*, Res. Astron. Astrophys. **23**, 075024 (2023).

[5] S. Chen, R. N. Caballero, Y. J. Guo, A. Chalumeau, K. Liu, G. Shaifullah, K. J. Lee, S. Babak, G. Desvignes, A. Parthasarathy *et al.*, Mon. Not. R. Astron. Soc. **508**, 4970 (2021).
[6] Z. Arzoumanian *et al.* (NANOGrav Collaboration), Astrophys. J. Lett. **905**, L34 (2020).
[7] B. Goncharov, R. M. Shannon, D. J. Reardon, G. Hobbs, A. Zic, M. Bailes, M. Curylo, S. Dai, M. Kerr, M. E. Lower *et al.*, Astrophys. J. Lett. **917**, L19 (2021).
[8] R. w. Hellings and G. s. Downs, Astrophys. J. Lett. **265**, L39 (1983).
[9] A. Afzal *et al.* (NANOGrav Collaboration), Astrophys. J. Lett. **951**, L11 (2023).
[10] S. Blasi, V. Brdar, and K. Schmitz, Phys. Rev. Lett. **126**, 041305 (2021).
[11] J. Ellis and M. Lewicki, Phys. Rev. Lett. **126**, 041304 (2021).
[12] R. Samanta and S. Datta, J. High Energy Phys. 05 (2021) 211.
[13] S. Datta, A. Ghosal, and R. Samanta, J. Cosmol. Astropart. Phys. 08 (2021) 021.
[14] R. Samanta and F. R. Urban, J. Cosmol. Astropart. Phys. 06 (2022) 017.
[15] D. Borah, S. Jyoti Das, R. Samanta, and F. R. Urban, J. High Energy Phys. 03 (2023) 127.
[16] J. Ellis, M. Lewicki, C. Lin, and V. Vaskonen, arXiv: 2306.17147.
[17] Z. Wang, L. Lei, H. Jiao, L. Feng, and Y. Z. Fan, arXiv: 2306.17150.
[18] N. Kitajima, J. Lee, K. Murai, F. Takahashi, and W. Yin, arXiv:2306.17146.
[19] G. Franciolini, A. Iovino, Jr., V. Vaskonen, and H. Veermae, arXiv:2306.17149.
[20] E. Megias, G. Nardini, and M. Quiros, arXiv:2306.17071.
[21] K. Fujikura, S. Girmohanta, Y. Nakai, and M. Suzuki, Phys. Lett. B **846**, 138203 (2023).
[22] C. Han, K. P. Xie, J. M. Yang, and M. Zhang, arXiv: 2306.16966.
[23] L. Zu, C. Zhang, Y. Y. Li, Y. C. Gu, Y. L. S. Tsai, and Y. Z. Fan, arXiv:2306.16769.
[24] P. Athron, A. Fowlie, C. T. Lu, L. Morris, L. Wu, Y. Wu, and Z. Xu, arXiv:2306.17239.
[25] J. Yang, N. Xie, and F. P. Huang, arXiv:2306.17113.
[26] S. Y. Guo, M. Khlopov, X. Liu, L. Wu, Y. Wu, and B. Zhu, arXiv:2306.17022; arXiv:2306.17158.
[27] Z. Q. Shen, G. W. Yuan, Y. Y. Wang, and Y. Z. Wang, arXiv: 2306.17143.
[28] V. K. Oikonomou, Phys. Rev. D **108**, 043516 (2023).
[29] G. Franciolini, D. Racco, and F. Rompineve, arXiv: 2306.17136.
[30] G. Lambiase, L. Mastrototaro, and L. Visinelli, arXiv:2306 .16977.
[31] T. Broadhurst, C. Chen, T. Liu, and K. F. Zheng, arXiv: 2306.17821.
[32] Y. Li, C. Zhang, Z. Wang, M. Cui, Y. L. S. Tsai, Q. Yuan, and Y. Z. Fan, arXiv:2306.17124.
[33] D. Borah, S. Jyoti Das, and R. Samanta, arXiv:2307.00537.
[34] E. Babichev, D. Gorbunov, S. Ramazanov, R. Samanta, and A. Vikman, arXiv:2307.04582.
[35] S. Vagnozzi, Mon. Not. R. Astron. Soc. **502**, L11 (2021).
[36] S. Bhattacharya, S. Mohanty, and P. Parashari, Phys. Rev. D **103**, 063532 (2021).
[37] S. Kuroyanagi, T. Takahashi, and S. Yokoyama, J. Cosmol. Astropart. Phys. 01 (2021) 071.
[38] M. Benetti, L. L. Graef, and S. Vagnozzi, Phys. Rev. D **105**, 043520 (2022).
[39] S. Vagnozzi, J. High Energy Astrophys. **39**, 81 (2023).
[40] A. Gruzinov, Phys. Rev. D **70**, 063518 (2004).
[41] T. Kobayashi, M. Yamaguchi, and J. Yokoyama, Phys. Rev. Lett. **105**, 231302 (2010).
[42] S. Endlich, A. Nicolis, and J. Wang, J. Cosmol. Astropart. Phys. 10 (2013) 011.
[43] D. Cannone, G. Tasinato, and D. Wands, J. Cosmol. Astropart. Phys. 01 (2015) 029.
[44] A. Ricciardone and G. Tasinato, Phys. Rev. D **96**, 023508 (2017).
[45] Y. F. Cai, J. O. Gong, S. Pi, E. N. Saridakis, and S. Y. Wu, Nucl. Phys. **B900**, 517 (2015).
[46] T. Fujita, S. Kuroyanagi, S. Mizuno, and S. Mukohyama, Phys. Lett. B **789**, 215 (2019).
[47] Y. Mishima and T. Kobayashi, Phys. Rev. D **101**, 043536 (2020).
[48] R. H. Cyburt, B. D. Fields, K. A. Olive, and T. H. Yeh, Rev. Mod. Phys. **88**, 015004 (2016).
[49] R. Abbott *et al.* (KAGRA, Virgo, and LIGO Scientific Collaborations), Phys. Rev. D **104**, 022004 (2021).
[50] B. P. Abbott *et al.* (LIGO Scientific and Virgo Collaborations), Phys. Rev. Lett. **118**, 121101 (2017); **119**, 029901(E) (2017).
[51] K. Bondarenko, A. Boyarsky, D. Gorbunov, and O. Ruchayskiy, J. High Energy Phys. 11 (2018) 032.
[52] M. Fukugita and T. Yanagida, Phys. Lett. B **174**, 45 (1986).
[53] E. K. Akhmedov, V. A. Rubakov, and A. Y. Smirnov, Phys. Rev. Lett. **81**, 1359 (1998).
[54] A. Pilaftsis and T. E. J. Underwood, Nucl. Phys. **B692**, 303 (2004).
[55] T. Hambye and D. Teresi, Phys. Rev. Lett. **117**, 091801 (2016).
[56] F. Vissani, Phys. Rev. D **57**, 7027 (1998).
[57] J. D. Clarke, R. Foot, and R. R. Volkas, Phys. Rev. D **91**, 073009 (2015).
[58] S. Blasi, V. Brdar, and K. Schmitz, Phys. Rev. Res. **2**, 043321 (2020).
[59] S. Datta and R. Samanta, J. High Energy Phys. 11 (2022) 159.
[60] A. Davidson, Phys. Rev. D **20**, 776 (1979).
[61] R. E. Marshak and R. N. Mohapatra, Phys. Lett. **91B**, 222 (1980).
[62] R. N. Mohapatra and R. E. Marshak, Phys. Rev. Lett. **44**, 1316 (1980); **44**, 1643(E) (1980).
[63] W. Buchmüller, V. Domcke, K. Kamada, and K. Schmitz, J. Cosmol. Astropart. Phys. 10 (2013) 003.
[64] A. D. Linde, Rep. Prog. Phys. **42**, 389 (1979).
[65] T. W. B. Kibble, Phys. Rep. **67**, 183 (1980).
[66] T. Han and X. Wang, J. High Energy Phys. 10 (2017) 036.
[67] See Supplemental Material at http://link.aps.org/supplemental/10.1103/PhysRevD.108.L091706 for a layman's description of the research, numerical equations to evolve the energy densities and computation of gravitational waves from cosmic strings.

[68] W. Zhao, Y. Zhang, and T. Xia, Phys. Lett. B **677**, 235 (2009).
[69] L. Page *et al.* (WMAP Collaboration), Astrophys. J. Suppl. Ser. **170**, 335 (2007).
[70] P. A. R. Ade *et al.* (BICEP2 and Keck Array Collaboration), Phys. Rev. Lett. **121**, 221301 (2018).
[71] A. R. Liddle and D. H. Lyth, Phys. Rep. **231**, 1 (1993).
[72] S. Kuroyanagi and T. Takahashi, J. Cosmol. Astropart. Phys. 10 (2011) 006.
[73] N. Seto and J. Yokoyama, J. Phys. Soc. Jap. **72**, 3082 (2003).
[74] L. A. Boyle and P. J. Steinhardt, Phys. Rev. D **77**, 063504 (2008).
[75] K. Nakayama, S. Saito, Y. Suwa, and J. Yokoyama, J. Cosmol. Astropart. Phys. 06 (2008) 020.
[76] S. Kuroyanagi, T. Chiba, and N. Sugiyama, Phys. Rev. D **79**, 103501 (2009).
[77] K. Nakayama and J. Yokoyama, J. Cosmol. Astropart. Phys. 01 (2010) 010.
[78] S. Kuroyanagi, T. Takahashi, and S. Yokoyama, J. Cosmol. Astropart. Phys. 02 (2015) 003.
[79] Y. Watanabe and E. Komatsu, Phys. Rev. D **73**, 123515 (2006).
[80] K. Saikawa and S. Shirai, J. Cosmol. Astropart. Phys. 05 (2018) 035; R. Abbott *et al.* (KAGRA, Virgo, and LIGO Scientific Collaborations), Phys. Rev. D **104**, 022004 (2021).
[81] N. Aghanim *et al.* (Planck Collaboration), Astron. Astrophys. **641**, A6 (2020); **652**, C4(E) (2021).
[82] A. Weltman, P. Bull, S. Camera, K. Kelley, H. Padmanabhan, J. Pritchard, A. Raccanelli, S. Riemer-Sørensen, L. Shao, S. Andrianomena *et al.*, Pub. Astron. Soc. Aust. **37**, e002 (2020).
[83] P. Amaro-Seoane *et al.* (LISA Collaboration), arXiv: 1702.00786.
[84] S. Kawamura, T. Nakamura, M. Ando, N. Seto, K. Tsubono, K. Numata, R. Takahashi, S. Nagano, T. Ishikawa, M. Musha *et al.*, Classical Quantum Gravity **23**, S125 (2006).
[85] B. Sathyaprakash, M. Abernathy, F. Acernese, P. Ajith, B. Allen, P. Amaro-Seoane, N. Andersson, S. Aoudia, K. Arun, P. Astone *et al.*, Classical Quantum Gravity **29**, 124013 (2012); **30**, 079501(E) (2013).
[86] S. Alekhin, W. Altmannshofer, T. Asaka, B. Batell, F. Bezrukov, K. Bondarenko, A. Boyarsky, K. Y. Choi, C. Corral, N. Craig *et al.*, Rep. Prog. Phys. **79**, 124201 (2016).
[87] A. M. Sirunyan *et al.* (CMS Collaboration), Phys. Rev. Lett. **120**, 221801 (2018).
[88] C. Ahdida *et al.* (SHiP Collaboration), J. High Energy Phys. 04 (2019) 077.
[89] D. Curtin, M. Drewes, M. McCullough, P. Meade, R. N. Mohapatra, J. Shelton, B. Shuve, E. Accomando, C. Alpigiani, S. Antusch *et al.*, Rep. Prog. Phys. **82**, 116201 (2019).
[90] M. Drewes, J. Hajer, J. Klaric, and G. Lanfranchi, J. High Energy Phys. 07 (2018) 105.
[91] A. Blondel *et al.* (FCC-ee study Team Collaboration), Nucl. Part. Phys. Proc. **273–275**, 1883 (2016).
[92] C. Ringeval, M. Sakellariadou, and F. Bouchet, J. Cosmol. Astropart. Phys. 02 (2007) 023.
[93] J. J. Blanco-Pillado, K. D. Olum, and B. Shlaer, Phys. Rev. D **83**, 083514 (2011).
[94] D. Matsunami, L. Pogosian, A. Saurabh, and T. Vachaspati, Phys. Rev. Lett. **122**, 201301 (2019).
[95] G. Agazie *et al.* (International Pulsar Timing Array Collaboration), arXiv:2309.00693.